RSC Advances

ROYAL SOCIETY OF CHEMISTRY

www.rsc.org/advances

Synthesis and lithium storage performances of Co_2SiO_4 Nanoparticles

Peisheng Guo and Chengxin Wang*

State Key Laboratory of Optoelectronic Materials and Technologies, School of Physics Science and Engineering, Sun Yat-sen (Zhongshan) University, Guangzhou 510275, People's Republic of China

Abstract

Herein, a method of synthesizing Co_2SiO_4 at a low temperature of 900 ^oC is reported. By synthesizing the precursor with a facile hydrothermal method and post-annealing in air under the temperature of 900 ^oC, the Co_2SiO_4 with good purity was attained. The Co_2SiO_4 nanoparticles were characterized by XRD, XPS and TEM to analyze their structure and morphology. When evaluating their performance as the anode materials for lithium ion battery, the Co_2SiO_4-based electrodes were investigated by cyclic voltammetry (CV), galvanostatic cycling and rate test. Such electrodes display superior electrochemical performances, such as providing large reversible capacity as high as 650 $mAhg^{-1}$ at the current density of 100 mAg^{-1} after 100 cycles, excellent cyclic performance and good rate capacity.

Keywords: cobalt silicate, low temperature, lithium ion battery

* Correspondence and requests for materials should be addressed to C. X. Wang.
Tel & Fax: +86-20-84113901
E-mail: wchengx@mail.sysu.edu.cn

1. Introduction

Since commercialized in the 1990-s by Sony Corporation[1], lithium-ion battery had witnessed the boom of consumer electronic devices, such as cell phone, lap-top computer and camera, just because of their high energy density, long cycle life and none memory effect[2-7]. Meanwhile, the revolution of electronic technology led to a growing demand for rechargeable batteries with larger capacity or reduced size and weight for a given capacity. What's more, with the development of electric vehicles (EVs) and hybrid electric vehicles (HEVs)[8,9], the graphite, whose specific capacity is ~372 $mAhg^{-1}$, cannot meet the constantly increasing demand for lithium ion battery with high energy density. Therefore, great efforts have been made to identify and research alternative anode materials with higher capacity and long term stability. Taking the anode materials into consideration, great attention has been attracted to the transition metal oxides because of their higher theoretic capacity. On the one hand, although great progress has been made in the transition metal oxides field[10], such as Mn_2O_3[11,12], Co_3O_4[13-15], they still face several challenges, including the rapid capacity fading, large volumetric change and poor cycle performance. On the other hand, because in the SiO/SiO_2 researches, the lithium silicate has been proved to be irreversible[16-19], the researchers do not focus on the transition metal silicates, which are abundant in the earth. Nevertheless, reversible conversion of the transition metal silicates was reported for the first time by Franziska Mueller in 2014[20]. In that report, the researchers synthesized the cobalt silicate by solid-state method and explored the mechanism of lithium insertion/extraction process.

Co_2SiO_4，which has good stability at high temperature, is widely used as the catalyst and magnetic materials[21]. Generally, Co_2SiO_4 is synthesized by a mean of the solid-state reaction, the temperature of which is too high. Morimoto et al[22]. synthesized the Co_2SiO_4 by heating the mixtures of Co_3O_4 and SiO_2 at the temperature as high as 1500 ^oC. Various methods have been taken to prepare the Co_2SiO_4 at low temperature, such as the precipitation method[23], the hydrothermal-reaction method[24] and sol-gel method[21]. Taguchi et al[24]. reported that Co_2SiO_4 can be synthesized by a hydrothermal reaction followed by calcination at 950 ^oC for 12h. Marcela Stoia et al[25]. claimed that Co_2SiO_4/SiO_2 composite can be obtained by a modified sol-gel method and the temperature is below 1000 ^oC.

In this paper, a method for the synthesis of Co_2SiO_4 is illustrated. In our work, the precursor was obtained by the hydrothermal reaction of hydrolytic amorphous SiO_2 and $C_4H_6O_4{\cdot}Co{\cdot}4H_2O$, then followed by calcination at 900 ^oC in air for 6h. Then, their excellent electrochemical performance was tested as anode materials for lithium ion battery. For example, the reversible specific capacity can reach 650 $mAhg^{-1}$, and the cycling stability and rate capability are promising.

2. Experimental Section

2.1 Sample preparation

Firstly, 5ml deionized water and 7mL ammonium hydroxide were added into 200mL ethyl alcohol, and then 7mL TEOS (Tetraethylorthosilicate) were added into the solution and magnetic stirring for 5h. The white powers were collected by

centrifugation, washed with ethyl alcohol and deionized water for several times, followed by dried at 80 ^{o}C for 12h. Secondly, 90mg hydrolytic amorphous SiO_2 was dissolved into 30 mL deionized water by sonication and magnetic stirring, and then 747mg Cobalt acetate tetrahydrate was added to the solution under magnetic stirring. After stirring, the red solution was transferred into a 50 mL Teflon-line autocalve and maintained at 180 ^{o}C for 24h. After being cooled to the room temperature naturally, the black powers were obtained by centrifugation, washed with deionized water and ethyl alcohol for several times, and dried at 70 ^{o}C for 12h. Finally, the precursors were calcined in air at 900 ^{o}C for 6h with a heating rate of 5 ^{o}C min^{-1} to obtain the purple powders.

1.2 Characterization

XRD patterns of the samples were recorded on a Rigaku D-MAX 2200 VPC with Cu Kα radiation at a generator voltage of 40 kV and current of 26 mA with a scanning speed of 5 deg min^{-1} from 10^{o} to 80^{o}. TEM observations were carried out on FEI Tecnai G2 F30 under 300 kV, Energy Dispersive X-ray Spectrometer (INCA300) mounted on the TEM, XPS (ESCALab250).

2.3 Electrochemical Characterization

Electrodes are the mixtures of active materials (Co_2SiO_4), binding agent (sodium carboxymethylcellulose) and conductive agent (acetylene black) in a weight ratio of 70:10:20. Then, the slurry was coated on a copper foil. After drying in air at 90 ^{o}C

for 12 h, the electrodes were assembled into coin-likes cells (CR2032) with pure lithium metal as both the counter electrode and the reference electrode, polypropylene micromembrane as the separator, 1M LiPF6 in ethylenecarbonate (EC) and diethyl carbonate (DEC) with a weight ratio of 1:1 as the electrolyte. The cells were assembled in an Ar-filled universal glove box with oxygen and water vapor pressure less than 0.3 ppm. Cyclic voltammetry (0.05-3.00 V, 0.1 mV s^{-1}) was performed using an electrochemical workstation (IM6e-X). The charge/discharge tests were performed using a NEWARE battery tester at different current rates with a voltage window of 0.005-3.0V.

3. Results and discussion

3.1 Structure and morphologies of Co_2SiO_4

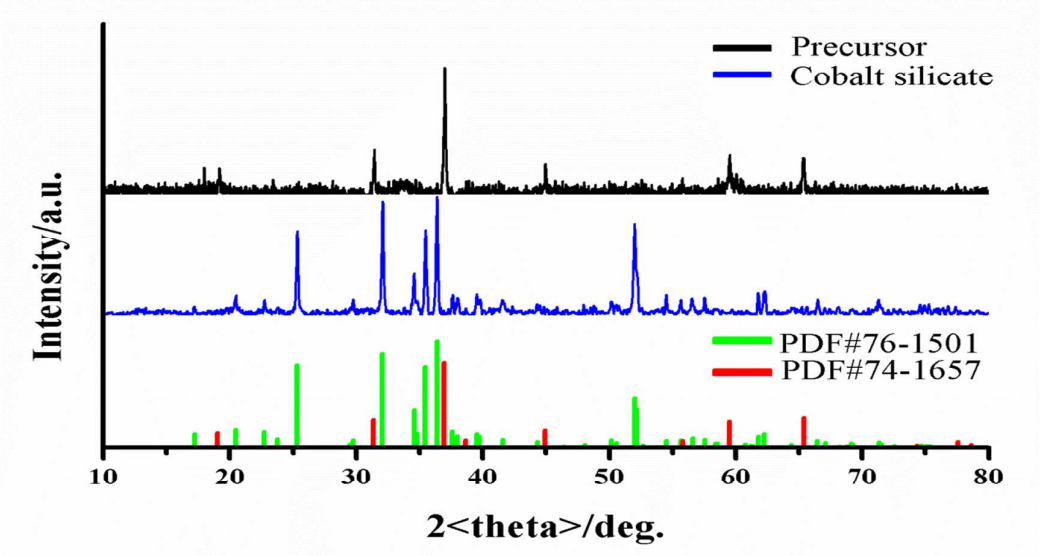

Figure 1 X-ray diffraction (XRD) pattern of as prepared precursor and Co_2SiO_4: as reference given in the bottom: JCPDS card no.76-1501 and JCPDS card no.74-1657.

Fig.1 shows the typical XRD pattern of the as-prepared precursor and Co_2SiO_4 samples. Before annealing, the XRD pattern of the precursor is well agree with the JCPDS card NO.74-1657, which shows that the precursor is Co_3O_4. The XRD pattern demonstrates that the structure of Co_3O_4 is cubic and the lattice constant is 0.8065 nm. After annealing at the the temperature of 900 ^oC, the sharpen peaks of the as prepared products XRD pattern indicate that the samples have good crystallization. What's more, comparing to the JCPDS references, all the peaks are in accordance with the card NO.76-1501, which shows that the as-synthesized products structure are orthorhobic and with the Pbnm space group. Different from other low- tempetature methods, the products have good purity, and no peaks of impurity can be observed from the XRD pattern. In the previous experients, the peaks of Co_3O_4 always can be detected when the temperature is below 1000 ^oC[21].

The product was investigated by X-ray photoelectron spectroscopy (XPS) to determine its chemical composition. The spectra recorded are shown in Fig.2. In the Co 2p spectrum, the peak of the Co $2p_{3/2}$ lies at 782.27 eV, which well matches with the Co^{2+} in the octahedral structure (781.9 eV)[26]. Besides, in the previous work, the binding energy of Co 2p in the Co_2SiO_4 structure is 781.3 eV[27], while the binding energy of Co 2p in Co_3O_4 is 779.6 eV[28]. Obviously, the binding energy of cobalt is closer to the former, which indicates that the products are Co_2SiO_4 instead of Co_3O_4. What is more, the energy separation between Co $2p_{1/2}$ and Co $2p_{3/2}$ for the products was 15.9 eV, which is closer to that of Co_2SiO_4 (Δ Co 2p=15.5eV)[29]. The formation of Co_2SiO_4 can be confirmed by analyzing the Si 2p core level spectrum (Fig.2 (c))

and the O 1s core level spectrum (Fig.2 (d)). The peak of the Si 2p localizes at the 102.79 eV, which indicates the formation of SiO_4^{4+} (the binding energy of Ni_2SiO_4 is 102.90 eV). What's more, the main peak of O 1s lie at 532.04 eV, which well demonstrates in the previous work[29]. Combined with the XRD and XPS analysis, the production can be predicted that the synthetic Co_2SiO_4 has good purity.

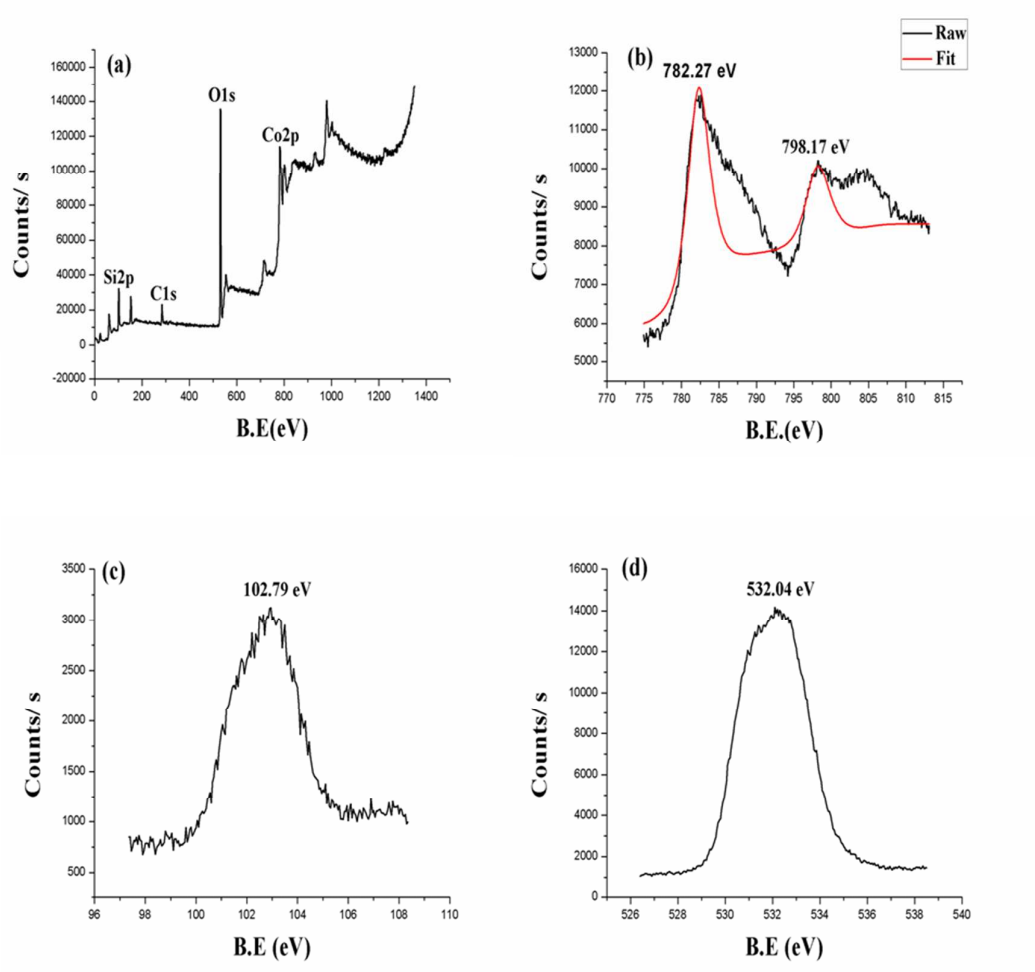

Figure 2. X-ray photoelectron spectroscopy of Co_2SiO_4: (a) the whole spectrum, (b) Co2p XP-spectrum, (c) Si2p XP-spectrum, (d) O1s XP-spectrum.

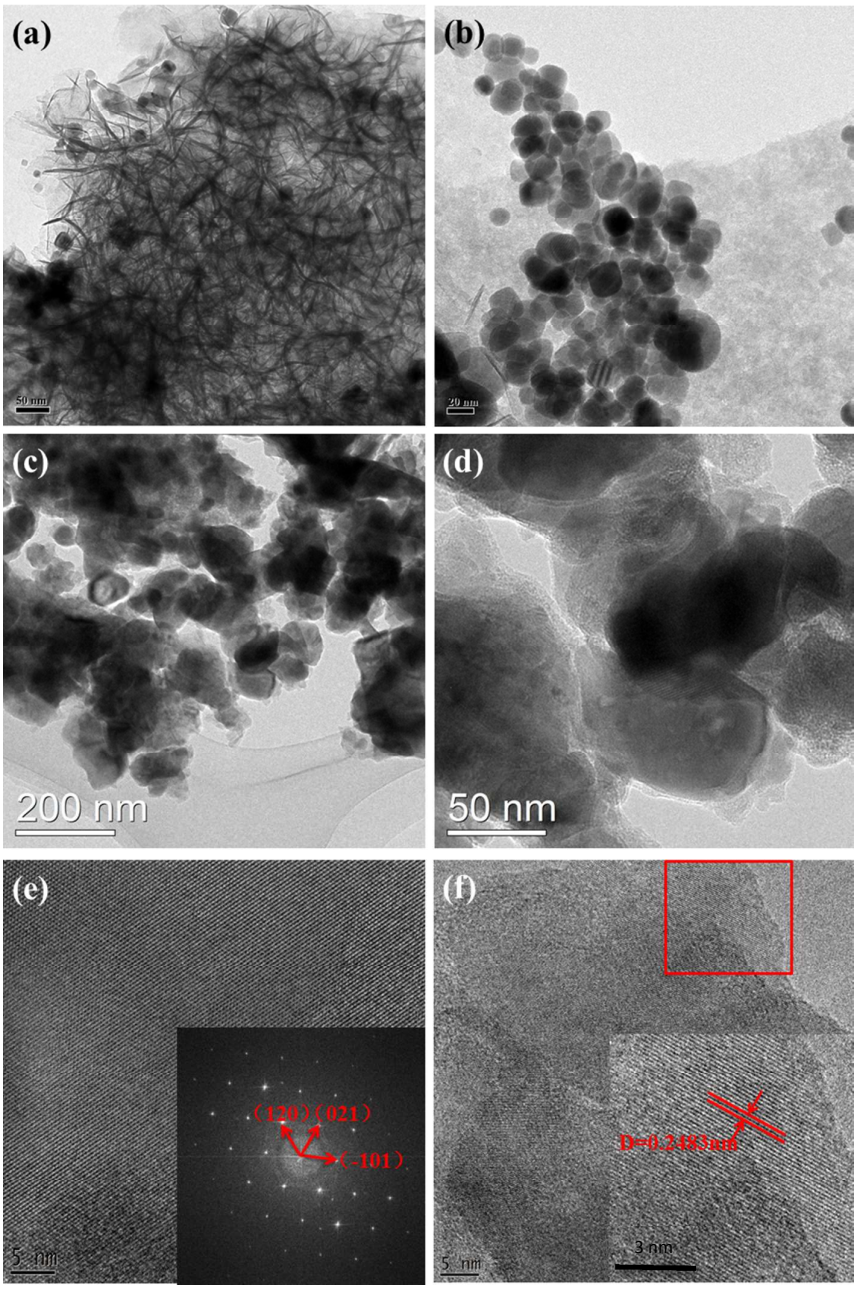

Figure 3 (a) and (b) the typical TEM images of precursors before annealing at different magnifications, (c) and (d) the typical TEM images of Co_2SiO_4 nanoparticles at different magnifications; (e) and (f) HRTEM images of Co_2SiO_4 nanoparticles, the inset in (e) is the corresponding FFT image of it, more details of (f) can be attained from inset of (f).

Fig.3 (a) and (b) show the typical transmission electron microscope (TEM) images of the precursor before calcination. The images show that the morphology of the precursor is mainly nanosheets (Fig. (a)) and the nanosheets interweave to form a bundle of agglomerated sheets. Meanwhile, a small amount of nanoparticles can be observed (Fig. 3 (b)). The presence of these particles suggested that the nanosheets yield is below 100%. Fig. 3(c) and (d) show the typical transmission electron microscope (TEM) images of the Co_2SiO_4 nanoparticles after calcination. The TEM images indicate that the as-prepared products have a predominantly nanoparticle morphology. Meanwhile, the sizes of the particles are various from several tens nanometers to 200 nanometers. However, some plate-like particles are also presented (supporting information Figure S1). From the TEM images, we can know that some nanosheets will be agglomerated and react with the particles to form the particle morphology and some of the nanosheets form the plate-like morphology independently when annealing at the temperature of 900 ^{o}C. Meanwhile, the existence of plate-like particles indicates that the morphology of Co_2SiO_4 nanoparticles is various.

The more details of the morphology can be attained from the HRTEM images. The HRTEM image of the nanoparticles is shown in Fig. 3 (e) and the corresponding FFT image was inserted in it. The HRTEM image indicates that the nanoparticles have good crystallization and the clearly lattice fringes can be observed. After calculation, the possible crystal faces are pointed in the FFT image with the red arrow. Furthermore, the HRTEM image of the plate-like particles in Fig. 3(f) displays a basal

space of 0.2483 nm, which is in good agreement with the (112) lattice fringe of orthorhombic Co_2SiO_4. At the same time, clearly layer structure can be observed. The plate-like particles are piled layer by layer. Moreover, the STEM image and corresponding mapping images of Co, Si and O (Fig.4 (a)-(d)) exhibit uniform distribution of Co_2SiO_4.

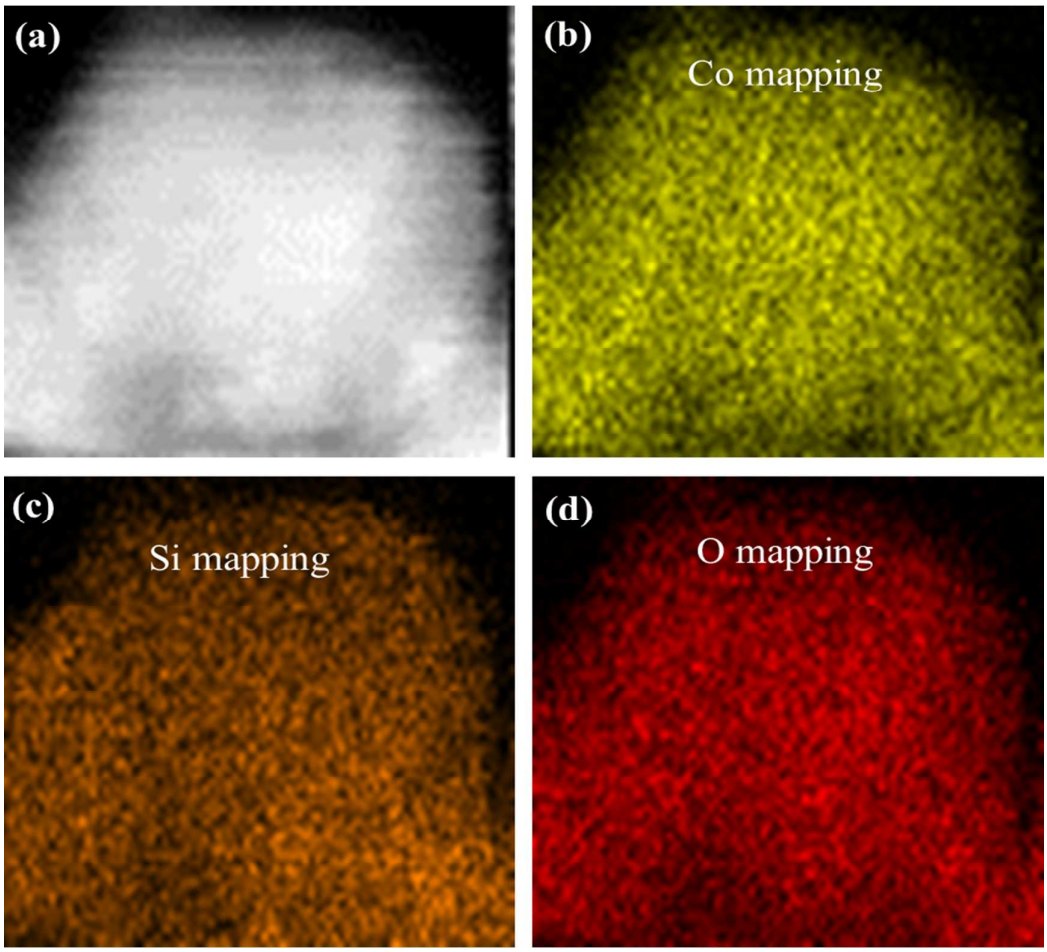

Figure 4 the mapping images of Co_2SiO_4 nanosheet: (a) STEM image, (b) Co mapping, (c) Si mapping and (d) O mapping.

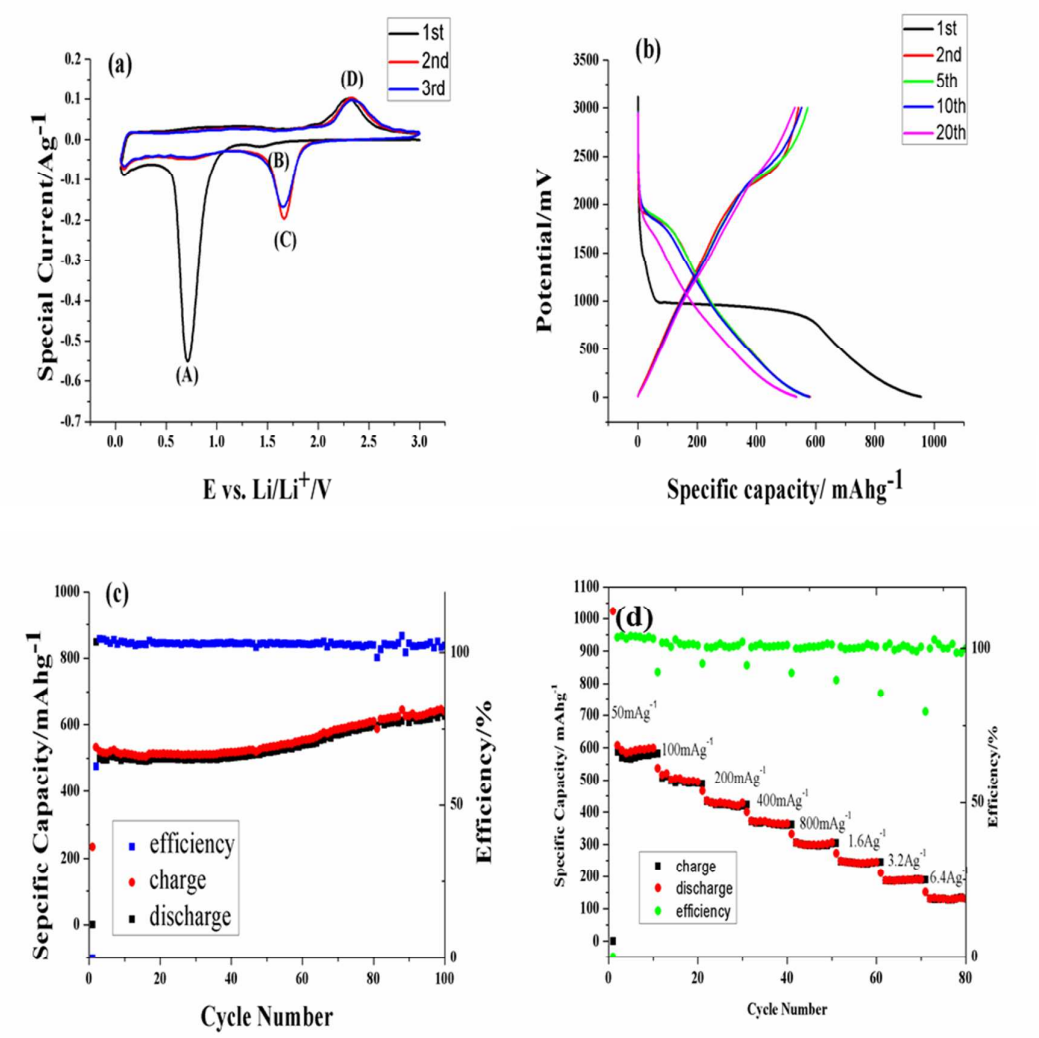

Figure 5 Electrochemistry performances of Co_2SiO_4: (a) Cyclic voltammetry (CV) of Co_2SiO_4-based electrodes: sweep rate: 0.1 mVs^{-1}, reversing potentials: 0.05V and 3.0V vs Li/Li^+. (b) the 1st, 2nd, 5th ,10th ,20th charge and discharge curves of the Co_2SiO_4-based anode materials at a current density of 50 mAg^{-1}. (c) galvanostatically tested at the current density of 100 mAg^{-1} for 100 cycles. (d) rate capability of the Co_2SiO_4 at various current densities between 50 mAg^{-1} and 6.4 Ag^{-1}.

Fig. 5 (a) shows the first three cyclic voltammograms (CVs) of the Co_2SiO_4-based electrode in the voltage range 0.05-3.0 V versus Li/Li^+ at the scan speed of 0.1mVs^{-1}. In the first cycle curve, two reduction peaks can be detected in the

cathodic sweep. The strong and obvious peak lied at (A) about 0.7 V, and the weak peak located at (B) around 1.4 V. While only one oxidation peak can be found in the anodic sweep and it located at about (D) 2.3 V. The XRD patterns of the Co_2SiO_4 electrodes at different voltages of the 1st lithiation (Fig.S2) show that the distinction between the voltage of 1.1 V and 2 V is not obvious. Considering the XRD analysis of Co_2SiO_4 electrodes, peak (B) is assigned to the small amount lithium ion insertion into crystalline structure for cobalt silicate to form the $Li_xCo_2SiO_4$, however, the lithium insertion didn't result in change of the Co_2SiO_4 lattice structure. This phenomenon is also shown in the previous report[30-32]. The peak (A), which only occurs in the initial cathodic sweep, results from the initial insertion into the crystalline of the lithium ion and the reduction of the transition metal[33]. In the following two cycles, the peak in the cathodic sweep can be detected in a same position, which is located at (E) around 1.7 V. The peak is assigned to the lithium ion insertion mechanism after the initial lithiation, which results in the structural reorganization[34,35]. Taking the anodic sweep into consideration, the peak (D) at ~ 2.3 V, is ascribed to the re-oxidation of cobalt metal, which is well matched with the researches on cobalt oxide[36,37]. At the meantime, the CV curves are coincident, which indicates the stable reversibility of the electrochemical reactions.

Fig.5 (b) illustrates the discharge-charge curves of Co_2SiO_4-based anode materials for lithium batteries at a current density of 50 mAg^{-1} at room temperature in a potential window between 0.005 and 3.0 V (versus Li^+/Li). In the first discharge curve, two plateaus can be observed, and the weak plateau lies at about 1.5 V, and the

obvious plateau locates at about 0.8-1.0 V. which is in good agreement with the cathodic peaks observed by cyclic voltammetry (Fig.5 (a)). After the potential plateau at 0.8-1.0 V, the discharge capacity of 955.7 $mAhg^{-1}$ can be attained. It is similar to the previous report[20] and can be owing to the decomposition of electrolyte[38]. Among the 2^{nd}, 5^{th}, 10^{th}, 20^{th} cycles, only one discharge slope is observed (in the range 1.6-2.0 V), with a decrease of discharge capacity. The discharge capacities of the electrode in the first, second, fifth, tenth, twentieth cycles are 955.6, 580.9, 576.3, 578.1, 535.7 $mAhg^{-1}$. Taking the charge curves into consideration, only one slope (in the range of 2.2-2.7 V) can be observed in all the curves, which matches well with the cyclic voltammetry and associated with the re-oxidation of cobalt metal.

Fig.5 (c) displays the discharge-charge capacity versus cycle number performance of Co_2SiO_4-based anodes. As can be seen, except for the first cycle, the capacity of the other ninety-nine cycles stays at a relative stable condition, which shows their good cycle stability. In the first fifty cycles, the capacity keeps as a constant at about 500 $mAhg^{-1}$, while in the next forty cycles, the capacity increases slowly and it can reach 650 $mAhg^{-1}$ after 100 cycles at 100 mAg^{-1}. The large capacity can be owing to the higher surface areas. From the image of Nitrogen adsorption/desorption isotherms and BJH pore size distributions of Co_2SiO_4 (Fig.S4), we can know that the pore is mesopore and its size is 7.0383 nm. The specific surface area of Co_2SiO_4 was 70.4040 m^2g^{-1}, and larger by 20 to 30 times than Co_2SiO_4 synthesized by Hideki Taguchi[24]. The larger surface area can facilitate Li ion insertion/extraction during the electrochemical reaction and shorten the pathways for

rapid lithium-ion and electron conduction[39]. The increase of the capacity may result from the reversible formation of polymeric layer on the Co_2SiO_4 particles, which matches well with the previous report[20]. What's more, once the increase capacity was attained, it can maintain upon continuous (dis)charge of the electrode and hold the high coulombic efficiency of about 99%, which indicates the Co_2SiO_4-based electrode have good stability and long cycle life.

To better understand the electrochemical behavior of the Co_2SiO_4-based electrodes, the rate performance with respect to the insertion/extraction of lithium ion was investigated. To exhibit its good rate performance, the Co_2SiO_4-based electrode is tested at various current densities (50--6400 mAg^{-1}) and the capacity and the coulombic efficiency are shown in Figure.5 (d). The cell shows good rate performance with reversible specific capacities of 590, 500, 430, 370 mAh^{-1} at current densities of 50, 100, 200 and 400 mAg^{-1}. What's more, while the current density changed back to 100 mAg^{-1}, the reversible specific capacity can be recovered as high as 560 $mAhg^{-1}$. The recovered capacity at the current density of 100 mAg^{-1} is much higher than the former, which may be resulted from the good lithium ion conductivity of the formation of lithium silicate[40]. Meanwhile, rate capacity of carbon coated Co_2SiO_4 was tested (Fig S3). The rate capacity of carbon coated Co_2SiO_4 shows better electrochemical performance, which could be owing to the carbon improve the conductibility of the Co_2SiO_4 particles.

4. Conclusions

Co_2SiO_4 nanoparticles were successfully synthesized by a facile hydrothermal method combining with a simple post-annealing process with low temperature, which can be synthesized at a large scale. With the respect to its application as the anode materials of lithium ion battery, the products were characterized structurally, morphologically and electrochemically. As the anode materials, the Co_2SiO_4-based electrodes exhibit good cycling retention, good rate performance and high specific capacity of 650 $mAhg^{-1}$ at a current density of 100 mAg^{-1} after 100 cycles. The excellent electrochemical performance indicates that the Co_2SiO_4 could be an alternative candidate as the active material for next-generation lithium ion battery.

Acknowledgements

This work was financially supported by the National Natural Science Foundation of China (51125008, 11274392, U1401241).

References:

1 Van Schalkwijk, W. & Scrosati, B. *Advances in lithium-ion batteries*. (Springer Science & Business Media, 2002).

2 Scrosati, B. & Garche, J. Lithium batteries: Status, prospects and future. *Journal of Power Sources* **195**, 2419-2430 (2010).

3 Scrosati, B. Recent advances in lithium ion battery materials. *Electrochimica Acta* **45**, 2461-2466, doi:http://dx.doi.org/10.1016/S0013-4686(00)00333-9 (2000).

4 Tarascon, J.-M. & Armand, M. Issues and challenges facing rechargeable lithium batteries. *Nature* **414**, 359-367 (2001).

5 Goriparti, S. *et al.* Review on recent progress of nanostructured anode materials for Li-ion batteries. *Journal of Power Sources* **257**, 421-443, doi:10.1016/j.jpowsour.2013.11.103 (2014).

6 Lu, L., Han, X., Li, J., Hua, J. & Ouyang, M. A review on the key issues for lithium-ion battery management in electric vehicles. *Journal of power sources* **226**, 272-288 (2013).

7 Marom, R., Amalraj, S. F., Leifer, N., Jacob, D. & Aurbach, D. A review of advanced and practical lithium battery materials. *Journal of Materials Chemistry* **21**, 9938-9954, doi:10.1039/C0JM04225K (2011).

8 Park, O. K. *et al.* Who will drive electric vehicles, olivine or spinel? *Energy & Environmental Science* **4**, 1621, doi:10.1039/c0ee00559b (2011).

9 Thackeray, M. M., Wolverton, C. & Isaacs, E. D. Electrical energy storage for transportation—approaching the limits of, and going beyond, lithium-ion batteries. *Energy & Environmental Science* **5**, 7854, doi:10.1039/c2ee21892e (2012).

10 Poizot, P., Laruelle, S., Grugeon, S., Dupont, L. & Tarascon, J. Nano-sized transition-metal oxides as negative-electrode materials for lithium-ion batteries. *Nature* **407**, 496-499 (2000).

11 Zhang, Y. *et al.* Facile synthesis of porous Mn2O3 nanoplates and their electrochemical behavior as anode materials for lithium ion batteries. *Chemistry-A European Journal* **20**, 6126-6130 (2014).

12 Hu, L., Sun, Y., Zhang, F. & Chen, Q. Facile synthesis of porous Mn 2 O 3 hierarchical microspheres for lithium battery anode with improved lithium storage properties. *Journal of Alloys and Compounds* **576**, 86-92 (2013).

13 Li, Y., Tan, B. & Wu, Y. Mesoporous Co3O4 nanowire arrays for lithium ion batteries with high capacity and rate capability. *Nano Letters* **8**, 265-270 (2008).

14 Zhan, F., Geng, B. & Guo, Y. Porous Co3O4 nanosheets with extraordinarily high discharge capacity for lithium batteries. *Chemistry* **15**, 6169-6174, doi:10.1002/chem.200802561 (2009).

15 Lou, X. W., Deng, D., Lee, J. Y., Feng, J. & Archer, L. A. Self-Supported Formation of Needlelike Co3O4 Nanotubes and Their Application as Lithium-Ion Battery Electrodes. *Advanced materials* **20**, 258-262, doi:10.1002/adma.200702412 (2008).

16 Miyachi, M., Yamamoto, H., Kawai, H., Ohta, T. & Shirakata, M. Analysis of SiO anodes for lithium-ion batteries. *Journal of the electrochemical society* **152**, A2089-A2091 (2005).

17 Yang, X., Wen, Z., Xu, X., Lin, B. & Huang, S. Nanosized silicon-based composite derived by in situ mechanochemical reduction for lithium ion batteries. *Journal of Power sources* **164**, 880-884 (2007).

18 Guo, B. *et al.* Electrochemical reduction of nano-SiO 2 in hard carbon as anode material for lithium ion batteries. *Electrochemistry Communications* **10**, 1876-1878 (2008).

19 Hwa, Y., Park, C.-M. & Sohn, H.-J. Modified SiO as a high performance anode for Li-ion batteries. *Journal of Power Sources* **222**, 129-134 (2013).

20 Mueller, F. *et al.* Cobalt orthosilicate as a new electrode material for secondary lithium-ion batteries. *Dalton transactions* **43**, 15013-15021, doi:10.1039/c4dt01325e (2014).

21 Cui, H., Zayat, M. & Levy, D. Effect of HCl on the PPO assisted sol-gel synthesis of olivine-type Co2SiO4 ultrafine particles. *Journal of Sol-Gel Science and Technology* **40**, 83-87, doi:10.1007/s10971-006-8216-y (2006).

22 Morimoto N, T. M., Watanabe M, Koto. Crystal structures of three polymorphs of Co2SiO4. *Am.Mineral.* **59**, 475 (1974).

23 Yatabe, J., Sugizaki, T., Ikawa, T. & Kageyama, T. Synthesis of Cobalt Silicate Using Water Glass as Raw Materials. *Journal of the Ceramic Society of Japan* **105**, 188-191, doi:10.2109/jcersj.105.188 (1997).

24 Taguchi, H., Takeda, Y. & Shibahara, H. Synthesis of olivine-type Co 1.6 SiO 4 at low

temperature. *Materials Letters* **52**, 412-416 (2002).

25 Stoia, M., Stefanescu, M., Dippong, T., Stefanescu, O. & Barvinschi, P. Low temperature synthesis of Co2SiO4/SiO2 nanocomposite using a modified sol–gel method. *Journal of Sol-Gel Science and Technology* **54**, 49-56, doi:10.1007/s10971-010-2156-2 (2010).

26 Ernst, B., Bensaddik, A., Hilaire, L., Chaumette, P. & Kiennemann, A. Study on a cobalt silica catalyst during reduction and Fischer–Tropsch reaction: in situ EXAFS compared to XPS and XRD. *Catalysis today* **39**, 329-341 (1998).

27 Okamoto, Y. *et al.* Preparation and characterization of highly dispersed cobalt oxide and sulfide catalysts supported on silica. *The Journal of Physical Chemistry* **95**, 310-319, doi:10.1021/j100154a057 (1991).

28 Moulder, J., Stickle, W., Sobol, P. & Bomben, K. Handbook of X-ray Photoelectron Spectroscopy. Perkin-Elmer Corporation, Physical Electronics Division (1992). *There is no corresponding record for this reference*.

29 Ming, H. & Baker, B. G. Characterization of cobalt Fischer-Tropsch catalysts I. Unpromoted cobalt-silica gel catalysts. *Applied Catalysis A: General* **123**, 23-36 (1995).

30 Xiao, W. *et al.* Fe2O3 particles enwrapped by graphene with excellent cyclability and rate capability as anode materials for lithium ion batteries. *Applied Surface Science* **266**, 148-154, doi:http://dx.doi.org/10.1016/j.apsusc.2012.11.118 (2013).

31 Jin, S. *et al.* Facile synthesis of hierarchically structured Fe3O4/carbon micro-flowers and their application to lithium-ion battery anodes. *Journal of Power Sources* **196**, 3887-3893, doi:http://dx.doi.org/10.1016/j.jpowsour.2010.12.078 (2011).

32 Wang, L., Yu, Y., Chen, P. C., Zhang, D. W. & Chen, C. H. Electrospinning synthesis of C/Fe3O4 composite nanofibers and their application for high performance lithium-ion batteries. *Journal of Power Sources* **183**, 717-723, doi:http://dx.doi.org/10.1016/j.jpowsour.2008.05.079 (2008).

33 Larcher, D., Sudant, G., Leriche, J., Chabre, Y. & Tarascon, J. The Electrochemical Reduction of Co3 O 4 in a Lithium Cell. *Journal of the Electrochemical Society* **149**, A234-A241 (2002).

34 Martinez-Julian, F. *et al.* Probing lithiation kinetics of carbon-coated ZnFe2O4 nanoparticle battery anodes. *The Journal of Physical Chemistry C* **118**, 6069-6076 (2014).

35 Bresser, D. *et al.* Carbon Coated ZnFe2O4 Nanoparticles for Advanced Lithium‐Ion Anodes. *Advanced Energy Materials* **3**, 513-523 (2013).

36 Li, W.-Y., Xu, L.-N. & Chen, J. Co3O4 nanomaterials in lithium‐ion batteries and gas sensors. *Advanced Functional Materials* **15**, 851-857 (2005).

37 Jayaprakash, N., Jones, W. D., Moganty, S. S. & Archer, L. A. Composite lithium battery anodes based on carbon@ Co 3 O 4 nanostructures: synthesis and characterization. *Journal of Power Sources* **200**, 53-58 (2012).

38 Ponrouch, A., Taberna, P.-L., Simon, P. & Palacín, M. R. On the origin of the extra capacity at low potential in materials for Li batteries reacting through conversion reaction. *Electrochimica Acta* **61**, 13-18 (2012).

39 Kim, S. J., Suk, J., Yun, Y. J., Jung, H. K. & Choi, S. Mesoporous silica-assisted carbon free Li2MnSiO4 cathode nanoparticles for high capacity Li rechargeable batteries. *Physical chemistry chemical physics : PCCP* **16**, 2085-2089, doi:10.1039/c3cp53436g (2014).

40 Xun, S. *et al.* The Effects of Native Oxide Surface Layer on the Electrochemical Performance of Si Nanoparticle-Based Electrodes. *Journal of The Electrochemical Society* **158**, A1260-A1266

(2011).

Contents Entry

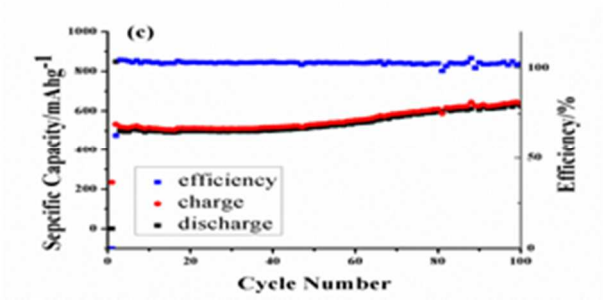

Synthesis cobalt orthosilicate at low temperature and their lithium storage performances are excellent.